2 mix

NASA TECHNICAL REPORT

NASA TR R-426

NASA TR R-426

(NASA-TR-R-426) LOW THRUST SPACE VEHICLE TRAJECTORY OPTIMIZATION USING REGULARIZED VARIABLES (NASA) 40 p HC $3.25 CSCL 22A

N74-20520

H1/30

Unclas
34335

APR 1974
RECEIVED
NASA STI FACILITY
INPUT BRANCH

LOW THRUST SPACE VEHICLE TRAJECTORY OPTIMIZATION USING REGULARIZED VARIABLES

by K. J. Schwenzfeger

George C. Marshall Space Flight Center

Marshall Space Flight Center, Ala. 35812

NATIONAL AERONAUTICS AND SPACE ADMINISTRATION • WASHINGTON, D. C. • APRIL 1974

1. REPORT NO.	2. GOVERNMENT ACCESSION NO.	3. RECIPIENT'S CATALOG NO.
NASA TR - 426		

4. TITLE AND SUBTITLE	5. REPORT DATE
Low Thrust Space Vehicle Trajectory Optimization Using Regularized Variables	APRIL 1974
	6. PERFORMING ORGANIZATION CODE
7. AUTHOR(S)	8. PERFORMING ORGANIZATION REPORT #
K. J. Schwenzfeger	M122
9. PERFORMING ORGANIZATION NAME AND ADDRESS	10. WORK UNIT NO.
George C. Marshall Space Flight Center Marshall Space Flight Center, Alabama 35812	11. CONTRACT OR GRANT NO.
	13. TYPE OF REPORT & PERIOD COVERED
12. SPONSORING AGENCY NAME AND ADDRESS	Technical Report
National Aeronautics and Space Administration Washington, D. C. 20546	14. SPONSORING AGENCY CODE

15. SUPPLEMENTARY NOTES

Prepared by Aero-Astrodynamics Laboratory, Science and Engineering.
This research was sponsored by a Postdoctoral Research Associateship through the National Academy of Sciences

16. ABSTRACT

Optimizing the trajectory of a low thrust space vehicle usually means solving a nonlinear two point boundary value problem. In general, accuracy requirements necessitate extensive computation times. In celestial mechanics, regularizing transformations of the equations of motion are used to eliminate computational and analytical problems that occur during close approaches to gravitational force centers. It was shown in previous investigations that regularization in the formulation of the trajectory optimization problem may reduce the computation time. In this study, a set of regularized equations describing the optimal trajectory of a continuously thrusting space vehicle is derived. The computational characteristics of the set are investigated and compared to the classical Newtonian unregularized set of equations. The comparison is made for low thrust, minimum time, escape trajectories and numerical calculations of Keplerian orbits. The comparison indicates that in the cases investigated for bad initial guesses of the known boundary values a remarkable reduction in the computation time was achieved. Furthermore, the investigated set of regularized equations shows high numerical stability even for long duration flights and is less sensitive to errors in the guesses of the unknown boundary values.

17. KEY WORDS	18. DISTRIBUTION STATEMENT
Low Thrust-Space Trajectories Trajectory Optimization Regularization	Cat. 30

19. SECURITY CLASSIF. (of this report)	20. SECURITY CLASSIF. (of this page)	21. NO. OF PAGES	22. PRICE
Unclassified	Unclassified	40	$3.25

MSFC - Form 3292 (Rev December 1972)

For sale by National Technical Information Service, Springfield, Virginia 22151

ACKNOWLEDGMENTS

The author would like to thank Dr. Hans Sperling of Marshall Space Flight Center's Aero-Astrodynamics Laboratory for giving the basic idea to this study and helping in many discussions, Mr. Roger Burrows of the Aero-Astrodynamics Laboratory for his valuable help in performing the numerical computations, and Mrs. Sarah Whitt for typing the original manuscript. The study was prepared during the author's participation in the NASA Post-doctoral Resident Research Associateship Program at the Marshall Space Flight Center.

TABLE OF CONTENTS

	Page
INTRODUCTION	1
PROBLEM FORMULATION	2
REGULARIZING TRANSFORMATION OF THE OPTIMIZATION PROBLEM	5
Derivation of the Regularized Equations	5
Use of Polar Coordinates	9
THE COAST ARC PROBLEM	11
Analytical Solution of the Coast Arc Problem	11
Numerical Calculations of Keplerian Orbits	13
MINIMUM TIME EARTH ESCAPE	15
Boundary Conditions	15
Discussion of Numerical Examples	17
CONCLUSIONS	23
APPENDIX A: AN ALTERNATE WAY TO DERIVE THE REGULARIZED EQUATIONS	24
APPENDIX B: SECOND-ORDER FORM OF LAGRANGIAN MULTIPLIER EQUATION $\bar{\lambda}_V$	27
APPENDIX C: INDEPENDENCE OF NEW SUBSTITUTED VARIABLES LIKE h AND $\bar{e}$	28
REFERENCES	31

LIST OF ILLUSTRATIONS

Figure	Title	Page
1.	Optimal low thrust earth escape spiral	18
2.	Real time compared to regularized time	18
3.	Optimal low thrust earth escape starting from a highly eccentric orbit	19
4.	Real time compared to regularized time	19

LIST OF TABLES

Table	Title	Page
1.	Comparison of the Numerical Integration Errors in Calculation of Keplerian Orbits with Different Sets of Equations of Motion	15
2.	Numerical Integration Characteristics for Different Types of Optimal Earth Escape Trajectories	17
3.	Convergence Characteristics of Different Kinds of Earth Escape Trajectories (λ_i Calculated by a Tangential Thrust Backward Integration).	21
4.	Initial Error Influence on the Convergence Characteristics of the 15.45 hr Earth Escape Spiral	22
5.	Initial Error Influence on the Convergence Characteristics of the 111 hr Earth Escape Trajectory	22

LIST OF SYMBOLS

Symbol	Dimension	Definition
e		Laplacian constant
F	N	thrust magnitude
h	m^2/sec^2	energy (Keplerian)
H		Hamiltonian
J		performance index
m	kg	vehicle mass
P	m/sec^2	disturbing acceleration
r	m	radius
s	sec/m	regularized time
t	sec	time
u		control variable, thrust direction
v	m/sec m^2/sec	velocity, regularized velocity
x		collecting symbol for all state variables
x, y, z	m	rectangular coordinates
Greek Symbols		
β	kg/sec	mass flow rate
φ	deg	central angle in x, y plane
λ_i		Lagrangian multiplier; subscript i indicates corresponding state variable
μ	m^3/sec^2	gravitational parameter γM, where γ is the gravitational constant and M is the mass of the central body

LIST OF SYMBOLS (Concluded)

Greek Symbols	Dimension	Definition
μ, ν		constant Lagrangian multipliers
θ	deg	out-of-plane angle
Other Symbols		
$(\cdot)$		time derivative
$(\,)'$		regularized time derivative
$\bar{a}$		indicates a as a vector
$\lvert\bar{a}\rvert$		absolute value of the vector a
$(\bar{a} \cdot \bar{b})$		inner product
$\bar{a} \times \bar{b}$		vector product

LOW THRUST SPACE VEHICLE TRAJECTORY OPTIMIZATION USING REGULARIZED VARIABLES

INTRODUCTION

The space vehicle trajectory optimization problem in general is treated from the point of view of the Mayer-Bolza problem which is well known in the calculus of variations [1,2]. Usually the solution must be obtained numerically, requiring some means of iteration procedures involving multiple integrations of sets of differential equations. One of the primary considerations in evaluating a numerical optimization procedure is the computation time for a predetermined accuracy with which the terminal conditions have to be satisfied. It is known that, when space vehicle trajectories cross regions with strongly varying gravitational force fields, the necessary numerical accuracy often requires extreme computation times. The computation time depends on (1) the numerical integration procedure, (2) the iterative numerical optimization method, and (3) the mathematical formulation of the problem used.

In this study, standard integration [3] and standard iteration [4,5] techniques are used. The main purpose of the investigation was to develop an improved formulation of the set of differential equations describing the space vehicle motion and the optimality conditions; in other words, to find a set of equations with high stability of numerical integration and less sensitivity with respect to errors in the required guesses for the unknown boundary conditions. These characteristics are necessary for the iteration procedure to demonstrate good convergence characteristics in isolating the optimal solution.

In celestial mechanics, regularizing transformations are used to remove the singularity which occurs due to the r^{-2} term in the equation of motion during close approach to a gravitational force center. These techniques reduce or eliminate computational and/or analytical problems in calculating those parts of space object trajectories [6]. It was shown in previous investigations [7,8,9] that the use of regularizing transformations in the formulation of the trajectory optimization problem may reduce the computation time and improve the convergence characteristics in comparison with unregularized sets of equations. Based on those results, in this study the equations for the optimal trajectory of a space vehicle with a continuous low thrust propulsion system are derived using regularized variables. The set of variables chosen was first described by Sperling [10] and Burdet [11]. The regularization for the state as well as for the Lagrangian multiplier equations is obtained by using only the classical Sundman [12] time transformation.

To investigate the numerical behavior of the derived system, example classes are chosen: first, numerical calculations of Keplerian orbits and, second, two-dimensional earth minimum time escape trajectories starting from various orbits and using various

vehicle characteristics. The results are compared in the first case with some other problem formulations and the analytical solution of Keplerian orbits and, in the second case, with the classical unregularized set of Newtonian equations of motion [6,8,13,14]. The comparison indicates that in the cases investigated, a reduction in computation time was achieved and that the regularized set of equations of motion is less sensitive to errors in the guesses of the unknown boundary conditions.

A complete analytical solution of the coast arc problem is presented. Some remarks on using the new, substituted, redundant variables h and e as independent state variables are given.

PROBLEM FORMULATION

The equation of motion of a spacecraft with a continuous thrusting propulsion system in an inverse-square gravitational force field can be written as

$$\ddot{\bar{r}} + \mu \frac{\bar{r}}{r^3} = \bar{P} \tag{1}$$

where $\bar{r}$ is the radius vector from the force center to the vehicle, which is assumed to be a point mass; r is the absolute value of the radius vector; $\mu = \gamma M$, where γ is the universal gravitational constant and M is the mass of the central body; and $\bar{P}$ is the vector of the thrusting acceleration defined as

$$\bar{P} = \frac{F}{m} \bar{u} \tag{2}$$

where F is the absolute value of the thrust, which is assumed to be constant in this study; $m = m_0 - \beta t$, the vehicle mass at time t with β as the constant mass flow rate; and $\bar{u}$ is the unit vector of the unspecified thrust direction.

The trajectory has to connect the given initial state

$$\bar{r}_0 = \bar{r}(t_0) \qquad \dot{\bar{r}}_0 = \dot{\bar{r}}(t_0) \qquad m_0 = m(t_0) \tag{3}$$

and the final state

$$\bar{r}_f = r(t_f) \qquad \dot{\bar{r}}_f = \dot{\bar{r}}(t_f) \tag{4}$$

The final time is either predetermined or free.

Then, the optimal transfer problem considered can be formulated as follows: Determine the unspecified thrust history $\bar{u}$ to minimize any performance index J, a function of the boundary values of the state $\bar{x}$, where $\bar{x}^T = (\bar{r}, \dot{\bar{r}}, m)$, and the time t:

$$J = J(\bar{x}_0, t_0, \bar{x}_f, t_f) \tag{5}$$

while satisfying the differential equations

$$\dot{\bar{x}} = f(\bar{x}, \bar{u}, t) \tag{6}$$

for $t_0 \leqslant t \leqslant t_f$ and the boundary conditions given in equations (3) and (4).

The necessary conditions for an optimal trajectory can be formulated as follows (e.g., see Reference 15). After introducing Lagrangian multipliers

$$\lambda_i = \lambda_i(t)$$

$$\mu = \text{constant} \quad , \tag{7}$$

the Hamiltonian of the system follows as

$$H(\bar{x}, \bar{\lambda}, \bar{u}, \mu) = \sum \lambda_i \dot{x}_i - \mu f \tag{8}$$

where f is the constraining equation of the control

$$f = (\bar{u} \cdot \bar{u}) - 1 = 0 \quad . \tag{9}$$

Thus, the Euler-Lagrangian equations are

$$\dot{x}_i = \frac{\partial H}{\partial \lambda_i} \, , \quad \dot{\lambda}_i = - \frac{\partial H}{\partial x_i}$$

$$\frac{\partial H}{\partial u_i} = 0 \tag{10}$$

and the Weierstrass condition is

$$H \, (\bar{x}_0, \, \bar{\lambda}, \, \bar{u}, \, 0) \leqslant H \, (\bar{x}_0, \, \bar{\lambda}, \, \bar{u}_0, \, 0) \tag{11}$$

for each $\bar{u}(t)$ which fulfills the constraint equation (9) and where $\bar{x}_0$ and $\bar{u}_0$ describe the optimum trajectory.

Combining equations (1), (2), (8), (10), and (11), the following differential equation system is derivable describing an optimal trajectory arc:

$$\ddot{\bar{r}} + \frac{\mu}{r^3} \, \bar{r} = \frac{F}{m} \, (t) \, \frac{\bar{\lambda}}{|\bar{\lambda}|}$$

$$\ddot{\bar{\lambda}} + \frac{\mu}{r^3} \, \bar{\lambda} = 3\mu \, \frac{(\bar{\lambda} \cdot \bar{r})}{r^5} \, \bar{r} \quad . \tag{12}$$

For a specific mission (e.g., earth escape, orbital transfer, etc.) the additional boundary conditions have to be considered.

Obviously, for impact trajectories $r \to 0$, both equations (12) for the state and the costate description contain a singularity. Even for close approach to a gravitational force center this singularity causes difficulties in numerical calculation of those trajectories. From this point of view it might be desirable to find a transformation of equations (12) that removes this singularity. In celestial mechanics, regularizing transformations are known which remove this singularity within the state equation. Applying those regularizing transformations to the optimal trajectory problem shows that

some of them will regularize the costate equation, too. In this investigation the well-known Sperling-Burdet variables and the classical Sundman time transformation are used. In future equations, system (12) is called "Newtonian Formulation" of the problem in contrast to the regularized form.

REGULARIZING TRANSFORMATION OF THE OPTIMIZATION PROBLEM

Derivation of the Regularized Equations

The derivation of regularized differential equations for the state variables and the Lagrangian multipliers can be approached either by regularizing the equations of motion and then setting down the necessary criteria for optimization in terms of the new independent variable or by setting up the complete optimization problem with ordinary time as the independent variable and then applying the regularizing transformation to the whole system of resulting equations. In the following derivation, the first approach is used. The second approach leads to the same set of equations, as is shown in Appendix A, for the second-order system of differential equations. The same connections are derived for a differential equation system of the first order by Czuchry and Pitkin [16].

Before applying the new independent variables, defined by the classical regularizing transformation of Sundman [12]

$$ds = r^{-1}\, dt \quad , \tag{13}$$

to the equations of motion, one may write equation (1) as

$$\begin{aligned} r^2\, \ddot{\bar{r}} &= -\dot{\bar{r}}\,(\bar{r}\cdot\dot{\bar{r}}) + 2h\,\bar{r} - \mu\,\bar{e} + r^2\,\bar{P} \\ \dot{h} &= (\dot{\bar{r}}\cdot\bar{P}) \\ \dot{\bar{e}} &= \frac{1}{\mu}\,[\dot{\bar{r}} \times (\bar{r} \times \bar{P}) + \bar{P} \times (\bar{r} \times \dot{\bar{r}})] \end{aligned} \tag{14}$$

where the following substitution equations for energy h and the Laplacian constant $\bar{e}$ and their time derivatives were used:

$$h = \frac{(\dot{\bar{r}} \cdot \dot{\bar{r}})}{2} - \frac{\mu}{r} \tag{15}$$

$$\bar{e} = -\frac{\bar{r}}{r} + \frac{1}{\mu}\left[\dot{\bar{r}} \times (\bar{r} \times \dot{\bar{r}})\right] \quad . \tag{16}$$

Because of equation (13), the transformation rule for a first-order derivative is

$$\frac{d(\cdot)}{dt} = \frac{1}{r}\frac{d(\cdot)}{ds} \qquad \text{[equation (13a)]}$$

and a second-order derivative is

$$\frac{d^2(\cdot)}{dt^2} = \frac{1}{r^3}\left[r\,\frac{d^2(\cdot)}{ds^2} - \frac{dr}{ds}\cdot\frac{d(\cdot)}{ds}\right] \quad . \qquad \text{[equation (13b)]}$$

Therefrom follows equation (17) for the second time derivative of the radius vector:

$$r^2\,\ddot{\bar{r}} = \bar{r}'' - \frac{(\bar{r} \cdot \bar{r}')}{r^2}\,\bar{r}' \quad . \tag{17}$$

Combining equations (13), (14), (17), and the differential equation of the mass variation $\dot{m} = \beta$ and transforming all first time derivatives with the aid of equation (13a) gives the complete set of regularized differential equations for the state variables. The radius vector equation appears in a second-order form.

Using the substitution $\bar{r}' = v$, the equations can be written in a first-order form:

$$\bar{r}' = \bar{v}$$

$$\bar{v}' = 2h\bar{r} - \mu\bar{e} + r^2\bar{P}$$

$$h' = (\bar{v} \cdot \bar{P}) \tag{18}$$

$$\vec{e}' = \frac{1}{\mu}\,[\bar{v} \times (\vec{r} \times \bar{P}) + \bar{P} \times (\vec{r} \times \bar{v})]$$

$$m' = \beta r \qquad \text{[(18) Concluded]}$$

$$t' = r$$

Setting up the Hamiltonian of system (18) and deriving its partial derivatives with respect to all of the state variables will lead to the following set of Lagrangian multiplier equations, the necessary conditions of optimality:

$$\bar{\lambda}_r' = -\bar{\lambda}_v 2h - (\bar{\lambda}_v \cdot \bar{P})2\bar{r} - [\bar{v} \times (\bar{\lambda}_e \times \bar{P}) + \bar{P} \times (\bar{\lambda}_e \times \bar{v})]/\mu - \lambda_m \beta \frac{\bar{r}}{r} - \lambda_t \frac{\bar{r}}{r}$$

$$\bar{\lambda}_v' = -\bar{\lambda}_r - \lambda_h \bar{P} + [\bar{r} \times (\bar{\lambda}_e \times \bar{P}) + \bar{\lambda}_e \times (\bar{r} \times \bar{P})]/\mu$$

$$\lambda_h' = (\bar{\lambda}_v \cdot \bar{r})2 \qquad (19)$$

$$\bar{\lambda}_e' = \bar{\lambda}_v \mu$$

$$\lambda_m' = -\frac{F}{m^2}\,|\bar{H}_P|$$

$$\lambda_t' = 0 \quad .$$

$|\bar{H}_P|$ is the absolute value of the partial derivative of the Hamiltonian H with respect to the thrusting acceleration P:

$$\bar{H}_P = r^2\,\bar{\lambda}_v + \lambda_h \bar{v} + \frac{1}{\mu}\,[\bar{r} \times (\bar{v} \times \bar{\lambda}_e) + \bar{\lambda}_e) \times (\bar{v} \times \bar{r})] \quad . \qquad (20)$$

The optimal thrust vector program is derived from the condition that the partial derivative of the Hamiltonian with respect to the control $\bar{u}$, which obeys the constraint equation

$$(\bar{u} \cdot \bar{u}) - 1 = 0 \quad , \qquad \text{[equation (9)]}$$

has to be zero. It follows that

$$\bar{u} = - \frac{\bar{H}_p}{|\bar{H}_p|} \quad . \qquad (21)$$

The sign in equation (21) follows from examining the second variation of the Hamiltonian with respect to $\bar{u}$ for minimization.

Equations (2), (18), (19), (20), and (21) give the complete set of equations for an optimal trajectory of a thrusting space vehicle in an inverse square force field. The system is completely regular for the state description. The equation for λ_r contains the unit vector of the radius $\bar{r}/r$ which has a well-known limit value for $r \rightarrow 0$ (e.g., see Reference 17).

Unfortunately the existence of this limit value, which makes the adjoint system regular as well as the state equations, does not prevent numerical difficulties in calculating trajectories which contain close approaches to a gravitational force center. For calculating plane trajectories the use of polar coordinates is advantageous because the adjoint system is completely regular (see following section). The increase of the number of differential equations is not an advantage with respect to the integration time. Compared to the classical formulation of the trajectory optimization problem [equations (12)] in the three-dimensional case, the number of equations increases from 7 to 12 for the state description and from 7 to 11 for the adjoint system, including the differential variation for the mass variation. Those additional equations are one vector equation for the Laplacian constant and two scalar equations for the energy and the time, which is now a new dependent variable. The adjoint system increases one equation less than the state system because the multiplier related to the time t is a constant, as is pointed out in Appendix A. If the time would appear explicitly in any of the equations (18) and (19), it always could be eliminated by using equation (7).

To calculate an optimal trajectory, it is only necessary to integrate 22 differential equations because of the linear connection between time and the mass variation. The equivalent numbers for the problem expressed in the K-S transformation [9] are 11 for the state and 10 for the multipliers. However, as shown by Tapley [18], the number of differential equations necessary to integrate when solving the optimization problem formulated in the K-S transformation is only 18.

With respect to the number of differential equations for two-dimensional trajectory calculations, the use of polar coordinates again may be advantageous because the number decreases to seven for the state description and to five for the adjoint system

(see following section). The integration interval changes from $t_0 \leqslant t \leqslant t_f$ to $s_0 \leqslant s \leqslant s_f$, with s_f unknown even in the case that t_f is given because s_f depends on the unknown history of the radius of the optimal trajectory [16].

In contrast to the classical set of equations for the optimal trajectory, the equation of the Lagrangian multiplier associated with the differential equation of the vehicle mass λ_m is not independent.

In Appendix B, a second-order form of the differential equation for $\bar{\lambda}_v$ is presented.

Use of Polar Coordinates

As pointed out in the previous section, the use of polar coordinates especially for calculating two-dimensional trajectories using the regularizing transformation presented may be advantageous.

Transforming equations (18) and (19) in polar coordinates gives the following set of equations for the state description:

$$
\begin{aligned}
r' &= v \\
v_r' &= 2hr + \mu + r^2 P_r \\
v_\varphi' &= r^2 P_\varphi \\
v_\theta' &= r^2 P_\theta \\
\varphi' &= v_\varphi/(r \cos\theta) \\
\theta' &= v_\theta/r \\
h' &= v_r P_r + v_\varphi P_\varphi + v_\theta P_\theta \\
m' &= \beta r \\
t' &= r
\end{aligned}
\qquad (22)
$$

and the following set for the adjoint system:

$$\lambda_r' = - \lambda_v 2(h + rP_r) - \lambda_{v_\varphi} 2rP_\varphi - \lambda_m \beta + \lambda_\varphi v_\varphi (r^2 \cos\theta)^{-1} + \lambda_\theta v_\theta r^{-2} - \lambda_{v_\theta} 2rP_\theta$$

$$\lambda_\varphi' = 0$$

$$\lambda_\theta' = - \lambda_\varphi v_\varphi \sin\theta \, (r \cos^2\theta)^{-1}$$

$$\lambda_{v_r}' = - \lambda_r - \lambda_h P_r$$

$$\lambda_{v_\varphi}' = - \lambda_h P_\varphi - \lambda_\varphi (r \cos\theta)^{-1} \qquad (23)$$

$$\lambda_{v_\theta}' = - \lambda_h P_\theta - \lambda_\theta r^{-1}$$

$$\lambda_h' = - \lambda_{v_r} 2r$$

$$\lambda_m' = - \frac{F}{m^2} |\bar{H}_P|$$

$$\lambda_t' = 0 \quad .$$

Obviously this system [equations (22) and (23)] is in a three-dimensional case not regularized. But in two-dimensions, it reduces to

$$r' = v_r$$

$$\varphi' = v_\varphi / r$$

$$v_r' = 2hr + \mu + r^2 P_r$$

$$v_\varphi' = r^2 P_\varphi \qquad (24)$$

$$h' = v_r P_r + v_\varphi P_\varphi$$

$$m' = \beta r$$

$$t' = r$$

and

$$\lambda_r' = - \lambda_{v_r} 2 (h + rP_r) - \lambda_{v_\varphi} 2r P_\varphi - \lambda_m \beta$$

$$\lambda_\varphi' = 0$$

$$\lambda_{v_r}' = - \lambda_r - \lambda_h P_r \qquad (25)$$

$$\lambda_{v_\varphi}' = - \lambda_h P_\varphi$$

$$\lambda_m' = - \frac{F}{m^2} |\bar{H}_P|$$

$$\lambda_t' = 0 \quad .$$

(H_p is defined in previous section.)

To solve the two-dimensional optimal trajectory problem, the equation system necessary to integrate is completely regular. It is only necessary to integrate 10 equations because the solution is independent of the central angle φ, the connection between mass and time is linear, and the Laplacian constant does not appear in the equations of motion. To determine the central angle, one additional integration is necessary after the optimization problem is solved.

THE COAST ARC PROBLEM

Analytical Solution of the Coast Arc Problem

A coasting arc is defined by setting the disturbing acceleration to zero. From equations (18) and (19) the following equations are obtained with $\bar{P} = 0$ and $\dot{m} = 0$:

$$\bar{r}'' - 2h_0 \bar{r}' + \mu \bar{e}_0 = 0$$

$$h' = 0$$

$$\bar{e}' = 0 \qquad (26)$$

$$m' = 0$$

$$t' = r$$

and

$$\bar{\lambda}_v'' - 2h_0\bar{\lambda}_v = 0$$

$$\lambda_h' = -2(\bar{\lambda}_v \cdot \bar{r})$$

$$\bar{\lambda}_e' = \mu \bar{\lambda}_v \qquad (27)$$

$$\lambda_m' = 0$$

$$\lambda_t' = 0 \quad .$$

h_0 $\bar{e}_0$ m_0 are defined by the initial conditions and remain constant over the whole arc. System (26), (27) assumes that the coast arc solution is independent of the time t and therefrom follows $\lambda_t = 0$.

Equations (26) are independent of equations (27). Both sets of equations (26) and (27) have an analytical solution. Equations (26) describe Keplerian orbits; they are used for numerical investigations in the following section.

In the case of $h_0 < 0$, elliptical motion, the solutions of equations (26) and (27) are

$$\bar{r} = \bar{a}\cos\omega s + \bar{b}\sin\omega s - \frac{1}{\omega^2}\mu\bar{e}_0$$

$$t = C_0 + C_1 s + C_2\cos\omega s + C_3\sin\omega s \qquad (28)$$

and

$$\bar{\lambda}_v = \bar{d}\cos\omega s + \bar{e}\sin\omega s$$

$$\bar{\lambda}_c = \frac{\mu}{\omega}(-\bar{e}\cos\omega s + \bar{d}\sin\omega s) + \bar{f} \qquad (29)$$

$$\lambda_h = f_0 + f_1 s + f_2 s^2 + f_3\sin\omega s + f_4\cos\omega s + f_5 s\sin\omega s + f_6 s\cos\omega s$$

with $\omega^2 = -2h_0$ and $\bar{a}$, $\bar{b}$, c_i, $\bar{d}$, $\bar{e}$, $\bar{f}$, f_i constants determinable from the initial conditions.

The solution of the hyperbolic case $h_0 > 0$ is similar using hyperbolic instead of trigonometric functions.

For $h_0 = 0$ parabolic case, the solutions of equations (26) and (27) are

$$\bar{r} = \frac{1}{2}\mu\,\bar{e}_0\,s^2 + \bar{g}_0\,s + \bar{g}_1$$

$$t = \int_{s_0}^{s_f} \sqrt{\alpha_0 + \alpha_1 s + \alpha_2 s^2 + \alpha_3 s^3 + \alpha_4 s^4}\,ds \tag{30}$$

and

$$\bar{\lambda}_v = \bar{k}_0 s + \bar{k}_1$$

$$\bar{\lambda}_e = \mu\left(\frac{1}{2}\,\bar{k}_0 s^2 + \bar{k}_1 s + \bar{k}_2\right) \tag{31}$$

$$\lambda_h = \ell_0 + \ell_1 s + \ell_2 s^2 + \ell_3 s^3 + \ell_4 s^4 + \ell_5 s^5 + \ell_6 s^6 \quad .$$

The constants $\bar{g}_0$, $\bar{g}_1$, α_i, $\bar{k}_0$, $\bar{k}_1$, $\bar{k}_2$, ℓ_i are functions of the initial conditions.

The solution for t is easily derivable as a sum of elliptical integrals of the first and the third kind (e.g., see Reference 19).

Formulations for the state variable equations of system (26) which allow simultaneous solutions of the system for all kinds of orbits may be found in the literature [20]. These formulations are adaptable for the multiplier equations (27), too (e.g., see Reference 9).

Numerical Calculations of Keplerian Orbits

The numerical calculation of Keplerian orbits is qualified as a test problem for the investigation of the numerical stability of the system [14] because a complete analytical solution is known. The accuracy of the numerical integration for short and long time orbits was compared with those of other regularized sets and the Newtonian unregularized set of trajectory equations presented in a paper of Baumgarte [13]. The sets compared are

1. Set N: The Newtonian equations

$$\ddot{\bar{r}} + \frac{\mu}{r^3}\bar{r} = 0 \quad . \qquad \text{[equation (1)]}$$

2. Set ST: A stabilized set (Baumgarte)

$$\bar{r}'' - \frac{1}{r^2}(\bar{r}\cdot\bar{r}')\bar{r}' + \left(\frac{1}{2r^2}|\bar{r}'|^2 + h\right)\bar{r}' = 0$$

$$t''' + 2ht' = \mu \quad . \qquad (32)$$

3. Set OCS: The oscillator equations (Stiefel, Scheifele K-S Transformation)

$$u_i'' + \frac{h}{2}u_i = 0$$

$$t' = u_1^2 + u_2^2 \quad . \qquad (33)$$

The transformation equations for the state x_1, x_2 (the coordinates of the radius vector in two dimensions) are $x_1 = u_1^2 - u_2^2$, $x_2 = 2u_1u_2$.

4. Set REG: Equations (12) with $\bar{P} = 0$

$$\bar{r}'' - 2h\bar{r} = -\mu\bar{e}$$

$$t' = r \quad . \qquad \text{[equations (26)]}$$

The unit system for numerical calculations is defined by $a = 1$, where a is the semimajor axis, and $\mu = 1$. The error in the distance due to numerical integration shown in Table 1 is defined as

$$\Delta = [(\Delta x_1)^2 + (\Delta x_2)^2]^{1/2}$$

$$\Delta x_i = x_{i\,\text{exact}} - x_{i\,\text{calculated}} \quad . \qquad (34)$$

TABLE 1. COMPARISON OF THE NUMERICAL INTEGRATION ERRORS IN CALCULATION OF KEPLERIAN ORBITS WITH DIFFERENT SETS OF EQUATIONS OF MOTION

Eccentricity E	2 Revolutions, Starting Point: Pericenter						1 Revolution, Starting Point: Apocenter					50 Revolutions			
	N[a]	ST	OSC	OSC[b]	REG	REG[b]	ST	OSC	OSC[b]	REG	REG[b]	ST	OSC	REG	REG[b]
0	7.7^{-6}	1.6^{-6}	1.7^{-7}	4.8^{-8}	1.6^{-6}	5.8^{-8}									
0.2	2.2^{-5}	1.2^{-5}	2.1^{-7}	4.8^{-8}	1.5^{-6}	5.7^{-8}									
0.6	1.2^{-2}	3.3^{-6}	3.4^{-7}	3.8^{-8}	1.3^{-6}	5.0^{-8}									
0.8	1.6	4.9^{-6}	5.1^{-7}	2.8^{-8}	9.8^{-7}	4.3^{-8}									
0.9							2.0^{-5}	7.5^{-7}	4.7^{-8}	3.6^{-7}	1.9^{-8}	5.3^{-4}	8.2^{-5}	1.7^{-5}	8.1^{-7}
0.95							1.5^{-5}	1.1^{-6}	4.8^{-8}	2.6^{-7}	1.8^{-8}	7.6^{-4}	1.2^{-4}	1.2^{-5}	8.1^{-7}
0.99							1.1^{-4}	2.6^{-6}	4.9^{-8}	1.2^{-7}	1.6^{-8}	5.3^{-3}	2.7^{-4}	5.9^{-6}	8.1^{-7}
0.999							7.6^{-1}	8.2^{-6}	4.9^{-8}	5.6^{-8}	1.6^{-8}				
0.999 999								5.3^{-5}	4.9^{-8}	4.3^{-8}	1.6^{-8}				

a. $(\ )^{-n}$ means $(\ ) \cdot 10^{-n}$

b. Integration performed with a Runge-Kutta procedure of the fifth-order with step size control.

For the numerical calculations, Runge-Kutta-Fehlberg [3] procedures of the fourth order with constant step size (as in Reference 16) and fifth order with step size control were used. The high stability of set REG is evident. The constant term $\mu\bar{e}$ in equation (26) produces stabilization in the long time calculations, even in comparison to the similar-looking oscillator-type equations (33).

MINIMUM TIME EARTH ESCAPE

Boundary Conditions

For the minimum time earth escape of the continuous thrusting vehicle with β the constant mass flow rate, the performance index was formulated as

$$J = (-m_f) \quad . \tag{35}$$

The only boundary condition at the final time is

$$h = 0 \quad . \tag{36}$$

Therefrom, an auxiliary function ϕ is constructed

$$\phi = - m_f + \nu h \quad . \tag{37}$$

The final values of the Lagrangian multipliers at the final time t_f with the definition $\lambda_i(t_f) = \lambda_{if}$ are

$$\begin{aligned} \lambda_{if} &= 0 \\ \lambda_{mf} &= -1 \\ \lambda_{hf} &= \nu \quad . \end{aligned} \tag{38}$$

The first equation of set (38) indicates that all final λ values, except λ_{mf} and λ_{hf} are zero. ν may be expressed in terms of the unknown state variables of the final time t_f using the condition that the Hamiltonian has to be equal to zero even at the final time. Using this condition and applying equations (38) gives

$$\nu = - \frac{|\beta| r_f m_f}{F |v_f|} \quad . \tag{39}$$

In deriving equations (38), it was assumed that energy h and Laplacian constant $\bar{e}$ can be considered as independent state variables. Independent is used in the sense that h and $\bar{e}$ are not functions of other state variables, i.e., the partial derivatives of ϕ [equation (37)] with respect to the radius and velocity are zero.

The question of the effect on the optimization problem of using additional (redundant) variables like h and $\bar{e}$ are not fully explored here. Some remarks concerning this problem are given in Appendix C.

Discussion of Numerical Examples

Equations (2), (18), (19), (20), and (21) and the boundary conditions (3), (36), and (38) form the complete set which is to be solved for the two-dimensional optimum escape trajectory calculation. The reason that the optimal trajectory is not determined by one integration of this set is that the state variables and multipliers are not given as a complete set at one definite time t. So the solution is an iteration process starting from any initial guess of the missing boundary values at the initial or final time. Usually, an initial guess of the Lagrangian multipliers is made.

In this study approximations of the initial values of the multipliers were determined from a backward integration of an escape trajectory using a tangential thrust program. This method made use of the knowledge that, for escape, a tangential thrust program is close to the optimal steering program. For the integrations, standard Runge-Kutta-Fehlberg [3] procedures of different orders as indicated in Tables 1 and 2 were used.

TABLE 2. NUMERICAL INTEGRATION CHARACTERISTICS FOR DIFFERENT TYPES OF OPTIMAL EARTH ESCAPE TRAJECTORIES

Trajectory Type	Set of Equations	Coordinate System	Max Error Per Step	Integr. Time Per Step (%)	No. of Steps	Error in H[b]		Quadratic Error[c]
						t_i	t_f	
Spiral	Newtonian	Rectangular	10^{-5}	100	52	$< 10^{-7}$	$< 10^{-8}$	$< 10^{-12}$
~3.7 Rev.	Regularized	Rectangular	10^{-5}	~200	37	$< 10^{-8}$	$< 10^{-7}$	$< 10^{-13}$
t_f = 15.45 hr	Regularized	Polar	10^{-4}	~100	24	$< 10^{-7}$	$< 10^{-9}$	$< 10^{-14}$
Spiral ~240 Rev. t_f = 35 days	Regularized	Polar	10^{-4}	~100	989	$< 10^{-6}$	$< 10^{-7}$	$< 10^{-12}$
Spiral ~700 Rev. t_f = 165 days	Regularized	Polar	10^{-4}	~100			$< 10^{-7}$	$< 10^{-12}$
Highly Ecc.	Newtonian	Rectangular	10^{-5}	100	26	$< 10^{-6}$	$< 10^{-7}$	$<10^{-13}$
t_f = 111 hr	Regularized	Rectangular	10^{-5}	~200	14	$< 10^{-6}$	$< 10^{-6}$	$<10^{-12}$
Highly Ecc.[a] t_f = 56 days	Regularized	Rectangular	10^{-4}	~100	132	$< 10^{-5}$	$< 10^{-8}$	$<10^{-13}$

a. Integration with Runge Kutta 4(5), all other cases with Runge Kutta 7(8) on MSFC's SDS 930 computer.
b. Hamiltonian of the system considered.
c. Sum of the quadratic errors in the boundary conditions at the time t_f.

The first example calculated is a 15.5 hour earth escape spiral from a low circular earth orbit with r = 1.05 times earth radius and an initial thrust to mass ratio of 0.1 m/sec^2. This example was also investigated in Reference 14. Although this t/m_0 is relatively large, it represents a compromise between a computationally expensive realistic trajectory and an inexpensive unrealistic trajectory. The optimal trajectory is shown in Figure 1 with the optimal thrusting angle measured against the path tangent.

Figure 2 shows the relationship between the new independent variable s, the regularized time, and the real time t.

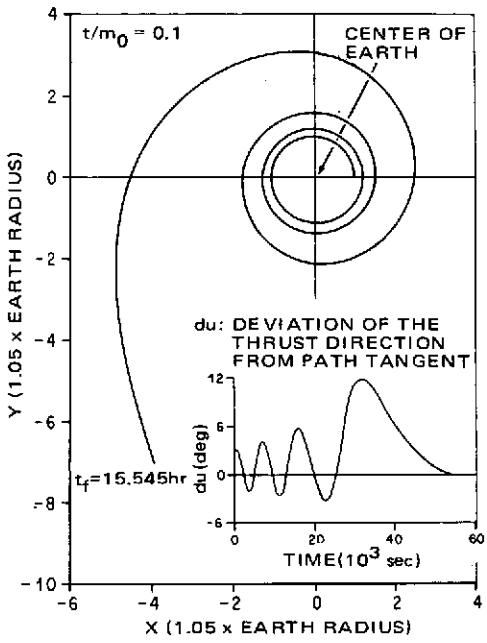

Figure 1. Optimal low thrust earth escape spiral.

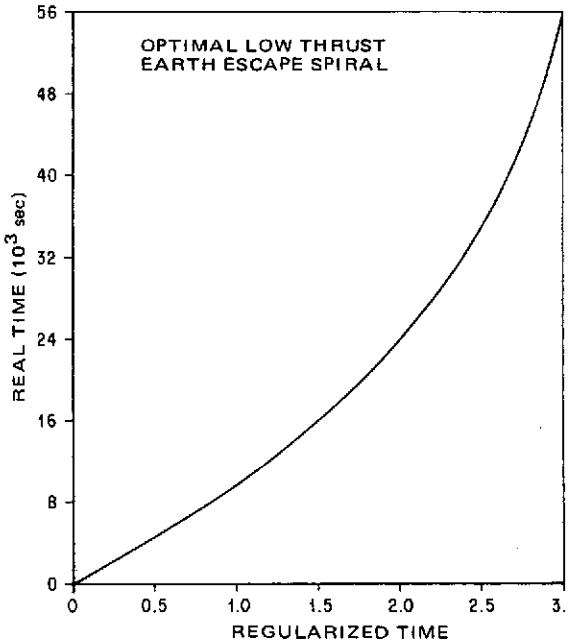

Figure 2. Real time compared to regularized time.

The second example investigated is shown in Figure 3. It is an optimal minimum time earth escape starting from a highly eccentric earth orbit near the earth with r_0 = 1.34 = earth radius. The gravitational force varies until the final time is reached by approximately a factor of 10^3 in magnitude; thus, it is expected that for certain error bounds the numerical integration step size will change within a wide range. The initial thrust to mass ratio of 3.10^{-3} m/sec^2 is somewhat more realistic than is the spiral escape. Figure 3 shows the optimal steering program. Figure 4 shows the relationship between the regularized time and real time. The spacecraft in both cases is considered as a point mass with a continuous thrusting device. The mass flow rate is constant. All examples are calculated in two dimensions.

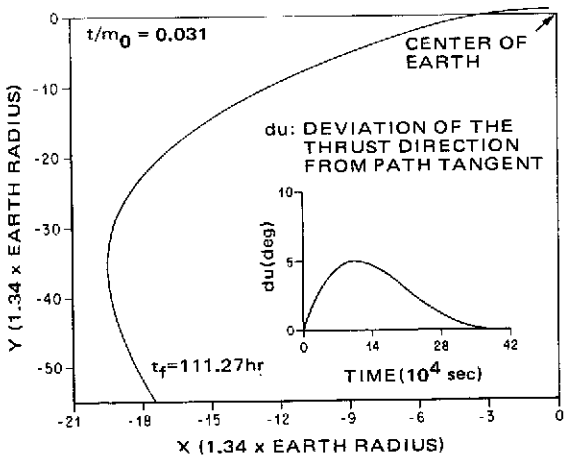

Figure 3. Optimal low thrust earth escape starting from a highly eccentric orbit.

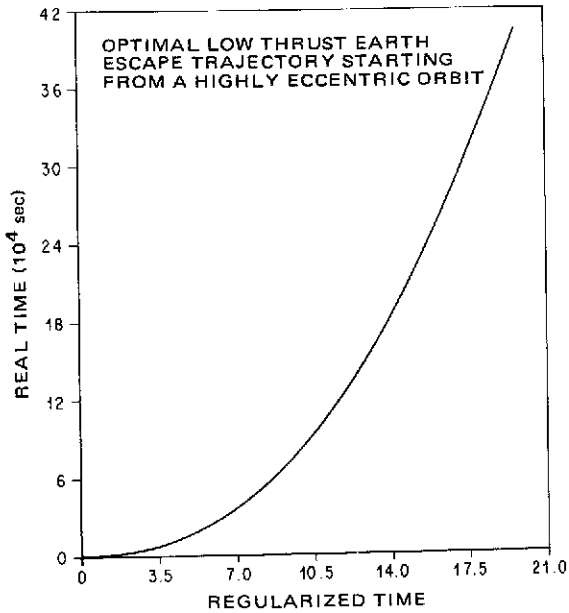

Figure 4. Real time compared to regularized time.

Table 2 gives some insight into the integration characteristics of the regularized set derived in comparison to the Newtonian set of equations of motion, which was also investigated in a first-order form. Some results, not shown in Table 2, indicate that the use of a second-order formulation of the Newtonian set of equations may save some integration time. It did not improve the convergence behavior of the system in those cases investigated.

The examples for the Newtonian set of equations were calculated in a rectangular coordinate system. For the regularized set of equations, rectangular and polar coordinates were used.

The integration time per step is given only in normalized form for comparison with the Newtonian case, which is chosen as 100 percent. The actual values for the SDS 930 used for the calculations are not representative of modern, faster computers (i.e., Univac 1108). The values given are based on a rough calculation from the duration of one complete trajectory integration divided by the number of steps. The number of step size changes is not considered but usually there was one additional step each time.

The doubling in the integration time per step for the regularized set in rectangular coordinates in comparison to the Newtonian set is essential due to the increased number of differential equations. That also explains the approximate equality of the integration time in the polar coordinates where the number of equations is equal to that of the Newtonian formulation.

The number of steps for the same error bound required in the boundary conditions at the final time is decreased by approximately 30 percent in the 15 hour spiral case and in the 111 hour escape case more than 40 percent as compared with the Newtonian set and the regularized set calculated in rectangular coordinates. The use of polar coordinates for this particular example seems advantageous, even when the number of steps is considered.

Since a closed form solution to the problem considered here does not exist, the error generated by the numerical integration process is unknown. The converged trajectory is always chosen as the optimal trajectory.

The error in the Hamiltonian given in Table 2 indicates that all calculations are made within the same error limits and gives an impression of the numerical accuracy achieved.

A certain control of the results is possible by comparing the final time with time necessary to achieve zero energy with a tangential thrust steering program. For each problem considered, the isolated trajectories calculated with different sets of equations and coordinate systems coincide at least within the number of digits indicated by the maximum allowable error per integration step.

The quadratic error given in the last column of Table 2 is defined as the sum of the quadratic error of the boundary conditions at the final time. The routine requires only that the value be smaller than 10^{-12}. The extent to which this criterion is exceeded is not controlled.

To demonstrate the numerical stability of the derived regularized set, three long duration optimal escape solutions are shown in Table 2. The 35-day spiral escape trajectory starts from a 1.05 earth radius circular orbit, with an initial thrust to mass ratio of 10^{-3} m/sec^2. The number of revolutions is more than 235. The 165 day spiral escape starts from the same circular earth orbit with an initial thrust to mass ratio of $5 \cdot 10^{-4}$ m/sec^2. The number of revolutions is more than 700. The 56-day escape trajectory starts from the highly eccentric orbit.

Table 3 shows the number of iterations and the number of trajectories calculated to isolate the optimal trajectory for all those cases listed in Table 2. The initial guesses of the unknown Lagrangian multipliers were in all cases systematically derived from a backward calculation starting from the final state, which was obtained from a tangential thrust steering program. The deviations of those λ values from the finally calculated optimal values differ depending on the individual sensitivity of those multipliers with respect to a nonoptimal steering program. The deviations range from 10 percent to about an order of magnitude and, most importantly, include changes in signs. Table 3 also shows the improved behavior of the regularized set in performing those calculations. The figures given are possibly not the best values attainable. The influence of different scaling systems or optimal selection of sensitivity factors for the optimization technique used is not considered for this comparison.

TABLE 3. CONVERGENCE CHARACTERISTICS OF DIFFERENT KINDS OF EARTH ESCAPE TRAJECTORIES (λ_i CALCULATED BY A TANGENTIAL THRUST BACKWARD INTEGRATION)

Type of Escape	Set of Equations	Coordinate System	Max Error Per Step	Quadratic Error	No. of Iterations	No. of Trajectories Calculated
Spiral 15.45 hr	Newtonian	Rectangular	10^{-5}	$< 10^{-12}$	19	26
	Regularized	Rectangular	10^{-4}	$< 10^{-12}$	6	16
	Regularized	Polar	10^{-4}	$< 10^{-13}$	4	11
Spiral 35 days	Regularized	Polar	10^{-4}	$< 10^{-12}$	30	37
Spiral 165 days	Regularized	Polar	10^{-4}	$< 10^{-12}$	18	25
Highly Ecc. 111 hr	Newtonian	Rectangular	10^{-5}	$< 10^{-12}$	29	36
	Regularized	Rectangular	10^{-4}	$< 10^{-15}$	6	16
Highly Ecc. 56 days	Regularized	Rectangular	10^{-4}	$< 10^{-13}$	13	23

The investigator was able to calculate the long duration cases only with the aid of the regularized set of equations of motion.

To investigate the sensitivity of the different sets of equations with respect to deviations of the initial λ values from the optimal values in Tables 4 and 5, the results of the non-realistic systematic changes in the initial λ's are given for the shorter escape cases. It is found that for small deviations due to the smaller number of differential equations, the Newtonian set may require less trajectory calculations than the regularized set; but for greater deviations the regularized set is obviously less sensitive. The remark "non-converged" indicates that after about 50 iterations, no improvement of the isolation procedure was noticed. Also, for the figures in Tables 4 and 5, no effort was made to derive the smallest possible number of iterations. For the sensitivity analysis, the error in the final time was always considered to be zero.

TABLE 4. INITIAL ERROR INFLUENCE ON THE CONVERGENCE CHARACTERISTICS OF THE 15.45 HR EARTH ESCAPE SPIRAL

$\alpha = \frac{\lambda_i}{\lambda_{opt}} \left(\frac{\text{initial } \lambda}{\text{optimal } \lambda} \right)$	Newtonian Set of Equations in Rectangular Coordinates		Regularized Set in Rectangular Coordinates	
	N[a]	n[c]	N	n
0.01	Not Conv.[b]		Not Conv.	
0.1	Not Conv.		21	31
0.5	17	24	8	18
0.8	7	14	5	15
1.0	0	1	0	1
1.2	7	14	6	16
2.0	16	23	16	26
10.0	19	26	20	30
100.0	Not Conv.		30	40

a. N - Number of iterations.
b. Not converged within 50 iterations.
c. n - Number of trajectories calculated to find the optimal solution.

TABLE 5. INITIAL ERROR INFLUENCE ON THE CONVERGENCE CHARACTERISTICS OF THE 111 HR EARTH ESCAPE TRAJECTORY

$\alpha = \frac{\lambda_i}{\lambda_{opt}} \left(\frac{\text{initial } \lambda}{\text{optimal } \lambda} \right)$	Newtonian Set of Equations in Rectangular Coordinates		Regularized Set in Rectangular Coordinates	
	N[a]	n[b]	N	n
0.1	Not Conv.		20	30
0.5	35	42	10	20
0.8	38	45	c	
1.0	0	1	0	1
1.2	20	27		
1.5	38	45	8	18
10.0	69	76	20	30

a. N - Number of iterations.
b. n - Number of trajectories calculated to find the optimal solution.
c. Not calculated.

CONCLUSIONS

Based on the results shown in this paper, the following conclusions may be drawn.

For the examples calculated, the integration time per trajectory necessary in the Newtonian and regularized formulations of the equations of motion are approximately equal. The gain due to the smaller number of steps using the regularized set is lost because of higher integration time per step which results from the use of a greater number of differential equations.

In the case of good initial guesses of the missing boundary values (i.e., the Lagrangian multipliers at the time $t = 0$), the smaller number of differential equations in the Newtonian formulation is even advantageous with respect to the numerical optimization method used. Only slight differences between both formulations were found.

On the other hand, a remarkable gain in computation time is achievable for the trajectory types investigated by using the regularized set in the more realistic cases of bad initial guesses for the Lagrangian multipliers. The smaller sensitivity of the regularized set leads more rapidly to the converged trajectory. In the case of extremely bad initial values, the regularized set gives the hope that convergence may be achieved where it otherwise may have been impossible.

In the long duration cases presented, convergence was achieved without use of aids other than those mentioned above and without major difficulties.

George C. Marshall Space Flight Center
National Aeronautics and Space Administration
Marshall Space Flight Center, Alabama, October 1973

APPENDIX A

AN ALTERNATE WAY TO DERIVE THE REGULARIZED EQUATIONS

Using the equation of motion [equation (1)] with the substitutions for energy h and Laplacian constant $\bar{e}$ that were made in equations (15) and (16) and the additional substitution of the velocity $\bar{v} = \dot{\bar{r}}$, one finds the first-order system of the equations of motion:

$$\begin{aligned}
\dot{\bar{r}} &= \bar{v} \\
\dot{\bar{v}} &= -\frac{1}{r^2}\left[\bar{v}\,(\bar{r}\cdot\bar{v}) - 2h\,\bar{r} + \mu\bar{e} - r^2\,\bar{P}\right] \\
\dot{h} &= (\bar{v}\cdot\bar{P}) \\
\dot{\bar{e}} &= \frac{1}{\mu}\left(\bar{v}\times(\bar{r}\times\bar{P}) + \bar{P}\times(\bar{r}\times\bar{v})\right) \\
\dot{m} &= \beta \quad .
\end{aligned} \tag{A-1}$$

If one starts setting up the optimization problem with the system (A-1) and using the time transformation dt = rds, one will not find the same set of Lagrangian multiplier equations (19). In particular, the system derived in such a manner will be more complex and not regularized, and the Lagrangian multiplier equation related to the differential equation of the vehicle mass will stay independent as in the classical case. However, starting from the second-order equation for the radius vector

$$r^2\,\ddot{\bar{r}} = -\,\dot{\bar{r}}\,(\bar{r}\cdot\dot{\bar{r}}) + 2h\,\bar{r} - \mu\bar{e} + r^2\bar{P} \tag{A-2}$$

and considering the fact that the regularized velocity using the time transformation dt = rds will be

$$\bar{v} = r\,\dot{\bar{r}} \quad , \tag{A-3}$$

the following first-order system will be derived:

$$\dot{r} = \bar{v}/r$$

$$\dot{\bar{v}} = (2h\,\bar{r} - \mu\bar{e} + r^2\bar{P})/r$$

$$\dot{h} = (\bar{v} \cdot \bar{P})/r \qquad \text{(A-4)}$$

$$\dot{\bar{e}} = \frac{\frac{1}{\mu}\,[\bar{v} \times (\bar{r} \times \bar{P}) + \bar{P} \times (\bar{r} \times \bar{v})]}{r}$$

$$\dot{m} = \beta \quad .$$

Starting with set (A-4) to set up the optimization problem gives the same Lagrangian multiplier equations as in the first approach described above.

The relation between ${}^{s}H$, the Hamiltonian of the regularized set of state equations (12), and ${}^{t}H$, the Hamiltonian of the unregularized set (A-4), is

$${}^{s}H = r\,{}^{t}H \quad . \qquad \text{(A-5)}$$

Building the partial derivatives gives the connection between the regularized and unregularized sets of multiplier equations:

$$\lambda_r' = \dot{\lambda}_r r - \frac{\bar{r}}{r}\,{}^{t}H = -\frac{\partial}{\partial \bar{r}}(r\,{}^{t}H) = -\frac{\partial {}^{s}H}{\partial \bar{r}}$$

$$\lambda_v' = \dot{\lambda}_v r$$

$$\lambda_h' = \dot{\lambda}_h r \qquad \text{(A-6)}$$

$$\lambda_e' = \dot{\lambda}_e r$$

$$\lambda_m' = \dot{\lambda}_m r \quad .$$

The second part of the first equation in set (A-6) appears because of the defining equation of the new independent variable. The additional multiplier λ_t follows for the autonomous system (18) and, as pointed out above, considering the necessary free boundary condition s_f as the constant,

$$\lambda_t = - {}^tH \quad . \tag{A-7}$$

${}^tH$ is the value of the Hamiltonian of the unregularized system (A-4) (see Reference 16).

APPENDIX B

SECOND-ORDER FORM OF LAGRANGIAN MULTIPLIER EQUATION $\bar{\lambda}_v$

The Lagrangian multiplier equations associated with the radius vector and velocity, equations (19), may be written as

$$\bar{\lambda}_r' = - 2h\bar{\lambda}_v - \frac{\partial \bar{H}_P}{\partial \bar{r}} \bar{P} + \lambda_m \beta \frac{\bar{r}}{r} + \lambda_t \frac{\bar{r}}{r} \tag{B-1}$$

and

$$\bar{\lambda}_v'' = - \bar{\lambda}_r' + \left(\bar{P} \cdot \frac{\partial \bar{H}_P}{\partial \bar{r}} \right)' \quad . \tag{B-2}$$

Finally, the second-order multiplier equation is

$$\bar{\lambda}_v'' - 2h\bar{\lambda}_v = \frac{\partial \bar{H}_P}{\partial \bar{r}} \bar{P} + \left(\frac{\partial \bar{H}_P}{\partial \bar{r}'} \cdot \bar{P} \right)' - (\lambda_m \beta + \lambda_t) \frac{\bar{r}}{r} \tag{B-3}$$

and the second-order radius equation remains

$$\bar{r}'' - 2h\bar{r} = - \mu \bar{e} + r^2 \bar{P} \quad . \tag{B-4}$$

The other equations for h', $\bar{e}'$, t', m', λ_h', $\bar{\lambda}_e'$, λ_t', λ_m' are unchanged [see equations (18) and (19)].

In comparison to the "Newtonian" Formulation, equations (12), the second-order multiplier equation for $\bar{\lambda}_v$ contains first-order derivatives on the right-hand side.

APPENDIX C

INDEPENDENCE OF NEW SUBSTITUTED VARIABLES LIKE h AND $\bar{e}$

Instead of systems (12) and (18), consider a simple optimization problem in general formulation.

Given is a differential equation system

$$\dot{x} = f(x, u, t) \tag{C-1}$$

and a definition equation

$$y = y(x, u, t) \quad . \tag{C-2}$$

Substituting y [equation (C-2)] into equation (C-1), the system of differential equations can be written as

$$\begin{aligned} \dot{x} &= f(x, y, u, t) \\ \dot{y} &= g(x, y, t) \quad . \end{aligned} \tag{C-3}$$

By introducing Lagrangian multipliers ${}^{x}\lambda$, ${}^{H}\lambda$, ${}^{y}\lambda$, where the left-hand superscript denotes to which of the state variables the adjoint variable is related, a function H (the Hamiltonian) can be defined for system (C-1):

$${}^{x}H = {}^{x}\lambda^{T} f \quad , \tag{C-4}$$

and for system (C-3):

$${}^{xy}H = {}^{x}\lambda^{T} f + {}^{y}\lambda^{T} g \quad . \tag{C-5}$$

(For distinction in setting down ${}^{xy}H$ for system (C-3) κ is used as a superscript for λ related to x instead of x as used for equation (34).

Using equation (C-4), the following differential equations for the multipliers ${}^{x}\lambda$ may be derived:

$$ {}^{x}\dot{\lambda} = - {}^{x}H_x = {}^{x}\lambda^T (f_x + f_y y_x) \tag{C-6} $$

where f is used as defined within the first equation of system (C-3) and y defined by equation (C-2). The right-hand side subscripts denote partial derivatives.

From equation (C-5), the following differential equations are derived.

$$ \begin{aligned} {}^{\kappa}\dot{\lambda} &= - {}^{xy}H_x = - {}^{\kappa}\lambda^T f_x - {}^{y}\lambda^T g_x \\ {}^{y}\dot{\lambda} &= - {}^{xy}H_y = - {}^{\kappa}\lambda^T f_y \quad . \end{aligned} \tag{C-7} $$

In order to show that system (C-6) is equivalent to system (C-7) while under consideration of

$$ g_x = (\dot{y})_x = (\dot{y}_x) \quad , \tag{C-8} $$

the first equation of system (C-7) is

$$ {}^{\kappa}\dot{\lambda} = - {}^{\kappa}\lambda^T f_x - {}^{y}\lambda(\dot{y}_x) + {}^{y}\dot{\lambda}^T y_x - {}^{y}\dot{\lambda}^T y_x \tag{C-9} $$

and the second equation of system (C-7) is

$$ {}^{\kappa}\dot{\lambda} = - {}^{\kappa}\lambda^T (f_x + f_y y_x) - ({}^{y}\lambda^T y_x) \quad . \tag{C-10} $$

Integrating the system (C-10) over t shows that the second part of the right-hand side of equation (C-10) is dependent on the boundary conditions only

$$\int_0^{t_f} ({}^{y}\lambda \dot{y}_x)\, dt = [{}^{y}\lambda y_x]_0^{t_f} \quad . \tag{C-11}$$

Thus, it follows that systems (C-7) and (C-6) are equivalent. They differ by an additive constant only.

The derivation of the equivalence of both Lagrangian multiplier systems shows that in both cases the same optimal arc will be derived using either this or the other formulation. It does show nothing about the influence on the procedure of calculating those optimum solutions carrying more, redundant, variables (as in this case y).

REFERENCES

1. Bliss, G. A.: Lectures on the Calculus of Variations. University of Chicago Press, Chicago, IL, 1946.

2. Lawden, D. F.: Optimal Trajectories for Space Navigations. Butterworths, London, 1963.

3. Fehlberg, E.: Classical Fifth-, Sixth-, Seventh-, and Eighth-Order Runge-Kutta Formulas with Stepsize Control. NASA TR R-287, Oct. 1968.

4. Burrows, R. R. and McDaniel, G. A.: A Method of Trajectory Analysis with Multi-Mission Capability and Guidance Applications. AIAA Guidance, Control and Flight Dynamics Conference, Pasadena, CA, Aug. 12-14, 1968.

5. Tapley, B. D. and Lewallen, J. M.: A Comparison of Several Numerical Optimization Procedures. Journal of Optimization Theory and Applications, vol. 1, no. 1, July 1967, pp. 1-33.

6. Stiefel, E. L. and Scheifele, G.: Linear and Regular Celestial Mechanics. Springer-Verlag, N. Y., Heidelberg, 1971.

7. Szebehely, V.; Pierce, D. A.; and Standish, S. M.: A Group of Earth to Moon Trajectories with Consecutive Collisions, Progress in Astronautics and Aeronautics: Celestial Mechanics and Astrodynamics, vol. 14, Edited by V. G. Szebehely, Academic Press, N. Y., 1964, pp. 35-51.

8. Tapley, B. D., et al,: Trajectory Optimization Using Regularized Variables. AIAA Journal, vol. 7, no. 6, June 1969, pp. 1010-1017.

9. Kocher, K.: Eine lineare Theorie der Optimierungsprobleme bei Raketen mit kleinem Schub. Dissertation, Eidgenoessische Technische Hochschule, Zürich, 1971.

10. Sperling, H.: Computation of Keplerian Conic Sections. ARS Journal, vol. 31, 1961, pp. 660-661.

11. Burdet, C. A.: Le mouvement Keplerien et les oscillateurs harmoniques. J für die reine u. angewandte Mathematik, 238, 1969.

12. Sundman, K. F.: Mémoire sur le problème des trois. corps. Acta Mathematica, vol. 36, 1912, pp. 105-179.

13. Baumgarte, J.: Numerical Stabilization of the Differential Equations of the Keplerian Motion. Celestial Mechanics, vol. 5, 1972, pp. 490-501.

REFERENCES (Concluded)

14. Lewallen, J. M., et al.: Coordinate System Influence on the Regularized Trajectory Optimization Problem. J. of Spacecraft and Rockets, vol. 8, no. 1, Jan. 1971. pp. 15-20.

15. Bryson, A. E. and Ho, Yu-Chi: Applied Optimal Control. Blaisdell Publishing Company, Waltham, Mass., 1969.

16. Czuchry, A. J. and Pitkin, E. T.: Regularization in Optimal Trajectory Problems. AIAA Journal, vol. 6, no. 6, June 1968, pp. 1209-1210.

17. Sperling, H. J.: The Collision Singularity in a Perturbed Two-Body Problem. Celestial Mechanics, vol. 7, 1969, pp. 213-221.

18. Tapley, B. D.: Regularization and the Calculation of Optimal Trajectories. Celestial Mechanics, vol. 2, 1970, pp. 313-333.

19. Byrd, P. F. and Friedman, M. D.: Handbook of Elliptical Integrals. Springer Verlag, Berlin, Gottingen, Heidelberg, 1954.

20. Stumpff, K.: Himmelsmechanik. VEB deutscher Verlag der Wissenschaften, Berlin, 1959.

NASA-Langley, 1974